2018 European Control Conference (ECC)
June 12-15, 2018. Limassol, Cyprus

SeaArm - A Subsea Multi-Degree of Freedom Manipulator for Small Observation Class Remotely Operated Vehicles

Ole Alexander N. Eidsvik[1], Bent Oddvar Arnesen[1] and Ingrid Schjølberg[1]

Abstract— **This paper presents the design of a novel low cost 4DOF fully electric subsea manipulator for small work class ROVs. The manipulator is designed to work on a wide range of typical observation class ROVs ranging from 5 kg and upwards. The small size makes the manipulator suitable to perform simple intervention tasks in addition to offering great mobility. The manipulator is designed to be completely modular. This again enables the arm to be reconfigured to fit size and performance requirement for a number of different applications. The functionality of the manipulator is tested in open water on a real ROV system. The manipulator performs remarkably. Despite the relative large size of the manipulator the overall response of the system is controlled and especially roll and pitch responses are smaller than one might expect. It is therefore shown that the hydrostatic restoring of the ROV is sufficient to stabilize the manipulator-ROV system without other sources of actuation.**

I. INTRODUCTION

Today a wide variety of Remotely Operated Vehicles (ROVs) are available from small observation class vehicles to large work class ROVs. The design of ROVs can typically be divided into three classes, work class, mid–class and observation class [1]. The main difference between these classes are that ROVs designed for observation usually have a limited payload capacity and the size is smaller than that of work class ROVs, usually less than 100kg. The mid-size class is usually referred to as "light work class" as they have limited payload options, but can be used for some intervention tasks. Work class ROVs on the other hand have the ability to carry a wide array of tools and sensors and can therefore perform interventions tasks such as maintenance, repair and installations. These are typically applied in the oil and gas industry. The market for small observation class ROVs has expanded rapidly in the later years. The number of producers has increased and the price has been reduced significantly. A limitation for these ROVs are their limited capability to perform interventions. They are usually limited to single-function gripper, grabbers or buckets, as more advanced manipulators have been too technically challenging and expensive to manufacture.

The challenges in designing a manipulator for small ROVs are many. Cost, power and weight are very important, but hydrodynamic properties such as drag, hydrodynamic mass, and buoyancy forces are also of great importance. All these challenges have been addressed during the design of this manipulator. Achieving a waterproof design, which can operate on depths of up to 100 meters, has also been proven a great challenge. Waterproof designs tend to increase the weight and cost of the components significantly. A custom-made waterproof system has therefore been developed and applied to this manipulator. The manipulator is powered by standard industry servos and all parts have been chosen from existing available commercial components, which makes maintenance and modification of the manipulator simple. The manipulator is tested with the BlueROV2 [2] to see how the manipulator performs when mounted on a small observation class ROV. Functional testing of the arm in air is also performed to ensure that the manipulator behaves as desired. For small observation class ROVs the operational limits will most likely be governed by the ROVs themselves rather than the manipulator. This because small ROVs usually have very limited hydrostatic restoring in both roll and pitch which makes them subjectable to large rotations in roll and pitch when moments are applied to the vehicles.

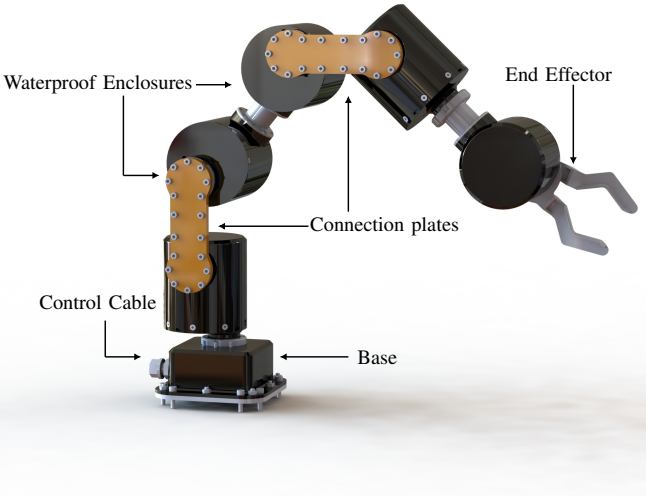

Fig. 1. Manipulator.

The work done on electrical subsea manipulators for small observation class ROVs are very limited. As most subsea manipulators today are hydraulic [3], multi degrees of freedom manipulators have been reserved for larger work class ROVs. Paredis et al. [4] proposed a modular multi degrees of freedom manipulator. The design allows the manipulator to easily be reconfigured by removing or adding joints. The manipulator is however not suitable for installation on small ROV systems due to the lack of waterproof design, large power requirements (72 V at 25 Amp) and large size.

[1]Centre for Autonomous Marine Operations and Systems, Department of Marine Technology, Norwegian University of Science and Technology, Trondheim, Norway

Matsumaru [5] suggested a similar modular manipulator design that can be assembled into any desired configuration. This modular design suffers from the same limitations as the one proposed by Paredis et al. [4] and is therefore not suitable for small ROVs. Rehman et al. [6] proposed a hydraulic manipulator design that solves the size and weight problem present on of the shelf hydraulic manipulators. The arm is however still too heavy for small ROVs with a weight in air of almost 30 kg. The arm is not water proof either which makes it unfeasible for subsea applications.

In recent years there have been an increasing interest in underwater snake robots (USR) [7][8] and a number of underwater snake robots have been developed such as the Amphibot III developed at Northeastern University[9] and the underwater snake robot Mamba developed at NTNU[10]. These robots are swimming underwater manipulators and therefore solves many of the problems regarding waterproof systems, such as weight and size. However these robots are expensive, require advanced control systems and are designed to operate without a ROV. Hence they can not rely on already existing systems. The proposed manipulator design have an advantage over USRs due to the fact that it is easy to use, control and install without the need for advanced sensors and other accessories. The cost of manufacture is also significantly less than that of USRs.

Research has also been performed on end-effector design. The end effector is perhaps the most important component of the manipulator, however it is not discussed in this work as the functionality of the manipulator itself is the focus.

This paper presents the design of a waterproof fully electric manipulator that can fit a wide range of ROV types. Combining electric drives and mechanics the underwater manipulator solves many problems regarding waterproof, lightweight and modular manipulator design. Hence the design presents an important contribution in the field of mechatronics. Another important contribution is the analysis of the hydrodynamic properties. The hydrodynamic properties of the manipulator is estimated using superposition and neglecting the interaction between the modules. Based on this analysis the importance of correctly positioning of the manipulator during ROV-transit is observed. Experimental tests are performed to verify the obtained results.

The outline of the paper is given in the following. Section II presents the manipulator design and specifications. A simple experimental test setup is described in Section III and the experimental results are presented in Section IV. Finally, Section V summarizes the concluding remarks.

II. Manipulator

A. Design

The main parameters for the manipulator are shown in Table I.

TABLE I

Manipulator specifications

Parameter	Value
Degrees of freedom	4
Material	Aluminium & stainless steel
Weight of Modules in air	0.424[kg]
Weight of Manipulator in air	2.4 [kg]
Submerged Weight	≈0 [kg]
Max reach (to end effector)	580.7 [mm]
Servos	5 x electric servos
Stall Torque at 14.8 V	10 [Nm]
Communication Protocol	Serial (8bit)

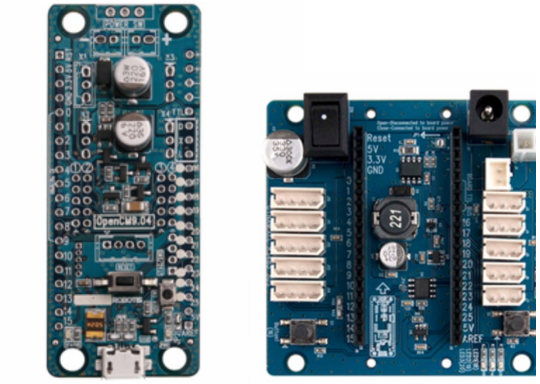

Fig. 2. CM 9.04 Microcontroller (left) and CM 485 Expansion board (right) [11].

The manipulator is built completely modular with identical modules to easily reduce or increase degrees of freedom. The modules are made up by a stainless steel cylinder sealed with an o-ring lid. Each module contains an electric servo that provides torque about the joint axis. The modules are connected through stainless steel hollow plates. These plates also serves the purpose of providing a waterproof connection for the servo cables. The plates can have arbitrarily lengths ranging from 10 cm to 50 cm which makes the length of the manipulator very easy to modify (the maximum length is governed by the maximum torque of the servo). The prototype presented in this work has 122 mm long connection plates which gives a maximum reach of 580.7 mm. The manipulator is rated to 100 meters water depth. The design can be modified to allow for larger depths, but this would require more robust connections between the joints. The stall torque of the servos are 8 [Nm], which translates to holding an object with a submerged weight of 2.4 kg horizontally (maximum torque occurs during the horizontal configuration). In air this limit is reduced to 1.3 kg as the manipulator must also carry its own weight. The servos are connected through a daisy chain, hence only one control cable is needed to control the manipulator. The control cable is connected to a CM 9.04 A-Type microcontroller using the CM 485 expansion board (Fig. 2). The manipulator is powered through an external battery source, which can either be the ROV's battery or an external power supply.

B. Kinematics

The kinematic relations for the manipulator depends on the chosen configuration. For the configuration used in this work the homogeneous transformation matrix for the manipulator can be found by taking the product of each joint-

TABLE II

DENVIT-HARTENBERG PARAMETERS [12]

i	α_{i-1}[rad]	a_{i-1}[mm]	d_i[mm]	θ_i[rad]
1	0	0	55.3	0
2	$-\pi/2$	0	0	$\theta_1 - \pi/2$
3	0	142.4	42.1	$-\pi/2$
4	$\pi/2$	142.4	0	$\theta_2 - \pi/2$
5	-$\pi/2$	0	13	π
6	$\pi/2$	0	42.1	$\theta_3 + \pi/2$
7	0	0	-139.6	$\pi/2$
8	0	59.6	-101	θ_4

transformation:

$$T_{base}^{effector} = T_0^1 T_1^2 T_2^3 T_3^4 T_4^5 \tag{1}$$

where the homogeneous transformation matrix from joint m to n is given by:

$$T_m^n = \begin{bmatrix} c(\alpha)c(\beta) & c(\alpha)s(\beta)s(\gamma) - s(\alpha)c(\gamma) & c(\alpha)s(\beta)c(\gamma) + s(\alpha)s(\gamma) & x_t \\ s(\alpha)c(\beta) & s(\alpha)s(\beta)s(\gamma) + c(\alpha)c(\gamma) & s(\alpha)s(\beta)c(\gamma) - c(\alpha)s(\gamma) & y_t \\ -s(\beta) & c(\beta)s(\gamma) & c(\beta)c(\gamma) & z_t \\ 0 & 0 & 0 & 1 \end{bmatrix} \tag{2}$$

The homogeneous transformation matrix consists of the 3x3 rotation matrix and the 3x1 homogeneous vector representing the coordinates. Inserting numerical values for the manipulator into Eq. (1) and (2) the transformation between the base and the end-effector is found. This transformation matrix is not shown here due to space constraints. A more convenient method for displaying the complete transformation matrix is to use the Denavit-Hartenberg(DH) convention [12]. The DH parameters for the manipulator are shown in Table II and the simplified sketch of the manipulator used for determining the parameters is shown in Fig. 3.

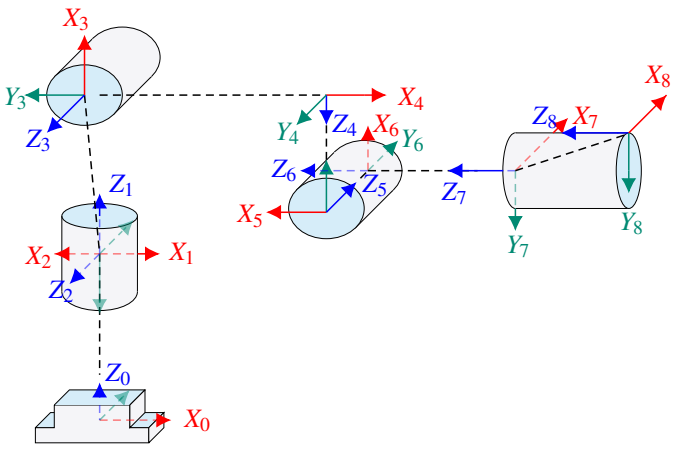

Fig. 3. Schematic representation of the coordinate-axes used for determining DH and homogenous transformation matrices.

C. Kinetics

The manipulator is designed for small observation class ROVs. These ROVs typically have a rigid body mass of about 10 kg. The manipulator's mass and hydrodynamic forces will therefore contribute significantly to the overall response of the system. The rigid body inertia forces for

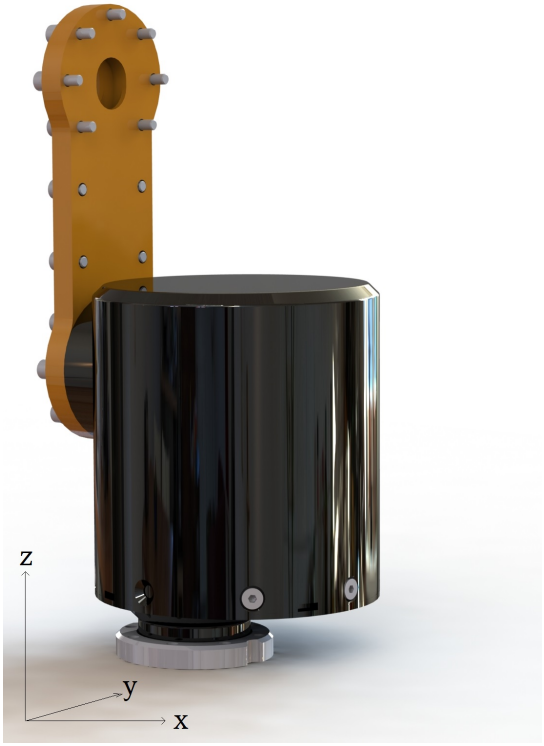

Fig. 4. Single module of Manipulator.

each module can easily be determined based on the rigid body mass of each module. The hydrodynamic forces on the other hand is quite difficult to determine with sufficient accuracy as both drag and added mass coefficients are functions of the joint angles and incoming flow conditions. Performing a simple CFD (Computational Fluid Dynamics) and BEM (Boundary Element Method) analysis, the drag and added mass for a single module can be estimated (Fig. 4). Neglecting the interaction between the modules, superposition can be used to obtain the hydrodynamic loads of the complete manipulator. This procedure introduces some errors as wake effects and structure interactions will have large effect on the hydrodynamic forces, but it should still give a reasonable estimate of the magnitude of the hydrodynamic forces. The hydrodynamic coefficients for one module can be seen in Table III. The base-module is for simplicity assumed to have the same hydrodynamic coefficients as the circular modules. The drag coefficients are estimated using SW Flow Simulation while the added mass coefficients are estimated using WADAM. Rotational drag and added mass forces are neglected. As previously stated, the manipulator is approximately neutrally buoyant. The modules were designed to be individually neutrally buoyant, hence the manipulator will remain neutrally buoyant regardless of the number of modules used i.e. degrees of freedom. The hydrostatic restoring of the manipulator following Archimedes' principle is therefore zero.

Based on the parameters in Table III the inertia and drag

TABLE III

HYDRODYNAMIC PARAMETERS FOR A SINGLE MANIPULATOR MODULE

Coefficient	Value
C_D^x	3.402 $[Ns^2/m^2]$
C_D^y	2.768 $[Ns^2/m^2]$
C_D^z	1.704 $[Ns^2/m^2]$
M_A^x	0.317 $[kg]$
M_A^y	0.312 $[kg]$
M_A^z	0.230 $[kg]$

forces and moments acting on a manipulator module can be estimated using Newton's 2nd law of motion:

$$\Sigma F = (M_A + M_{RB})\dot{\nu} + (C_D)\nu|\nu| \tag{3}$$

where ν is the velocity vector of each module in an inertial reference frame, M_A is the added mass matrix, M_{RB} is the rigid body mass matrix and ΣF is the resulting forces and moments. Assuming fixed joint angles and purely horizontal response the total forces and moments on the manipulator base can be calculated based on Eq. (3). For the case where the manipulator is fixed vertically i.e. joint angles are:

$$\theta_1 = 0,\ \theta_2 = \pi/2,\ \theta_3 = 0,\ \theta_4 = 0$$

Eq. (3) becomes:

$$M = 1.24\dot{\nu} + 4.69\nu|\nu| \tag{4}$$

where M is the moment acting on the manipulator base. From Eq. (4) it can be observed that for even modest accelerations and velocities the base-moment becomes significant. As most small observation class underwater vehicles have limited hydrostatic restoring in roll and pitch this added moment can produce severe roll and pitch angles for the underwater vehicle. Eq (4) and (5) are only valid given zero rotation of the ROV and is hence an idealized scenario. The torque produced on the base will in reality give the ROV a rotation which will introduce Coriolis and centripetal forces in addition to varying the inflow velocity on the manipulator. Assuming the manipulator is fixed in a horizontal position in-line with the velocity and acceleration the base-moment can be reduced significantly. A strictly horizontal position translates to all joint angles being equal to zero (see Fig. 3)

$$\theta_n = 0 \quad for \quad n = 1:4$$

The corresponding base-moment becomes:

$$M = 0.65\dot{\nu} + 2.46\nu|\nu| \tag{5}$$

The base-moment is hence reduced by 50% simply by aligning the manipulator inline with the direction of the motion. This shows the importance of correctly positioning and orienting the manipulator during ROV-operations.

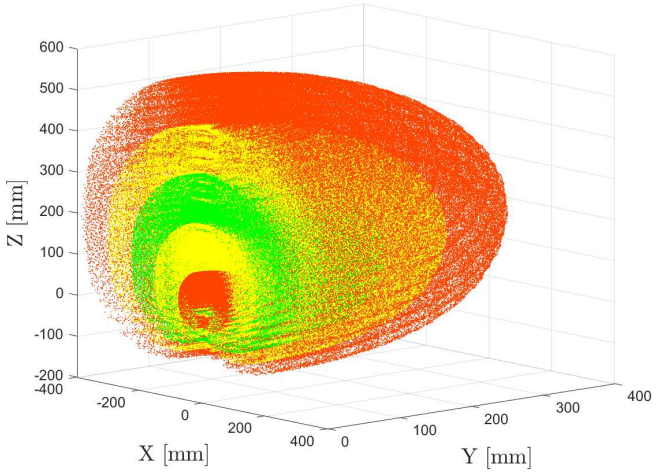

Fig. 5. Scatter plot of manipulator work space. Color ranging from green to center of workspace to red at the boundaries.

D. Workspace

The workspace for the manipulator is determined using a brute force approach. Based on the kinematic relations presented in the previous subsection the obtainable end effector positions are calculated using forward kinematics. This translates to checking different combinations of joint angles to obtain a 3D scatter plot of obtainable positions. For this purpose the following algorithm is used:

- $\theta_1, \theta_2, \theta_3$ and θ_4 are set to their minimum limit.
- The angles are increased by interval of 0.1 rad pr. iteration using a quadruple for-loop.
- The corresponding end deflection is found from Eq. (2).
- The end deflections are stored in an array of obtainable positions.

Fig. 5 shows the scatter plot obtained by using the aforementioned algorithm (note that only positive values of y-direction is included due to symmetry about the XZ-plane).

III. EXPERIMENTAL TEST SETUP

A. Laboratory

The experimental testing is performed in the Marine-Cybernetics laboratory (MC-lab) at NTNU (Fig. 6). MC-lab is a 40 meters long, 6.45 meters wide and 1.5 meters deep towing tank. The tank is equipped with a towing carriage, planar motion mechanism (PMM), wave maker and a current generator. For the tests performed in this work the Qualisys motion capture system were not available due to other activities in the laboratory. All measurements were therefore taken from the on board sensors of the ROV.

B. BlueROV2

The experimental platform used to verify the functionality of the manipulator is the small observation class ROV BlueROV2. BlueROV2 is produced by BlueRobotics and the

Fig. 6. Marine Cybernetics Laboratory.

TABLE IV
BLUEROV2 SPECIFICATIONS

Parameter	Value
L,H,W	457 [mm], 338 [mm], 254 [mm]
Weight in Air	11 [kg]
Thrusters	T-200
Battery	14.8 [V], 10 [Ah]
Maximum Forward Speed	1 [m/s]
Submerged Weight	-0.2 [kg]
Max Rated Depth	100 [m]
Sensors	Gyroscope, Accelerometer, Magnometer and Barometer
Onboard Computer	Raspberry Pi 3
Control System	M Robotics Pixhawk

main specifications are shown in Table IV. The manipulator is connected to the ROV's own internal power supply which is a 14.8 V, 10 Ah battery. The manipulator is connected directly to the battery using an 8 Amp Universal Battery Eliminating Unit (UBEC) supplying 12 V.

The manipulator is mounted on the underside of the ROV, directly below the center of gravity (COG). The ROV has a small offset in pitch due to a horizontal offset between the center of buoyancy (COB) and center of gravity (COG). This offset is a result of the tether, extra instruments installed and sub-optimal placing of ballast elements. However the offset does not affect the maneuverability of the ROV. In Fig. 7 and 8 the manipulator is shown mounted on the BlueROV2 and the offset in pitch can clearly be seen.

C. Communication

Communication between the user and manipulator takes place through the same communication interface that has been developed between user and the BlueROV2. This interface is known as the Mission Oriented Operating Suite (MOOS), originally developed by Paul Newman at MIT [13]. MOOS uses a database called MOOSDB, acting as a central server application communicating through publish and subscribe protocols in a star-like topology. The communication between the user and both manipulator and ROV can be seen in Fig. 9. Commands are sent as strings from the computer

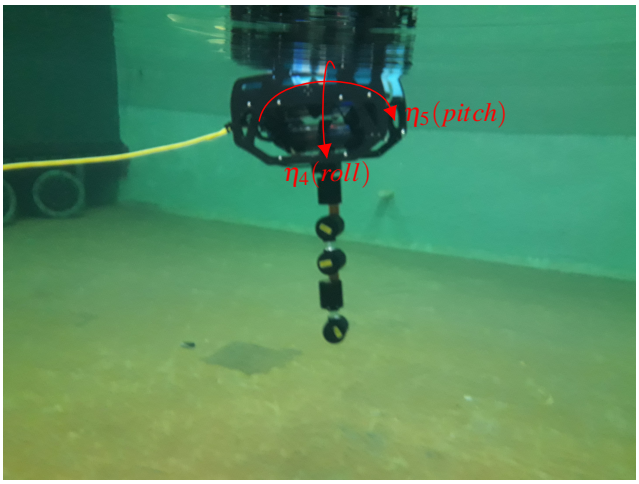

Fig. 7. Manipulator mounted on BlueROV2. The manipulator is positioned vertically.

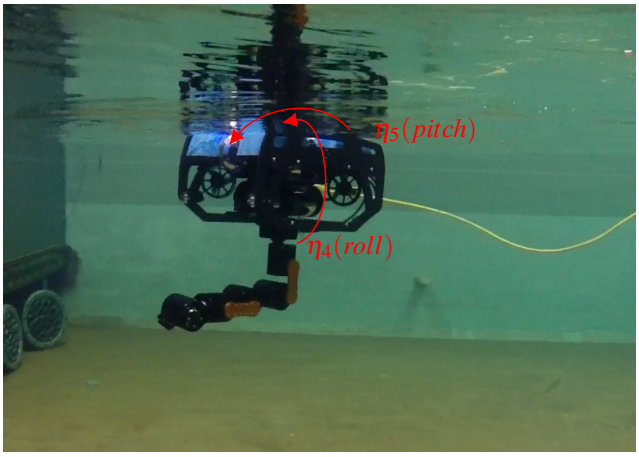

Fig. 8. Manipulator mounted on BlueROV2. The manipulator is positioned horizontally facing forwards.

through the ROV's ethernet tether to MOOSDB by a python script. The Raspberry Pi 3 (RPi3) located inside the vehicle launches another python script that subscribes for changes in MOOSDB. These changes are passed through the USB (serial) to the OpenCM9.04 microcontroller. Finally, C-code on the OpenCM handles manipulator command strings and converts the string type values to doubles, which are fed as commands to the servos of the manipulator.

D. Test Procedure

The test procedure is designed to test whether the ROV is able to maneuver with the manipulator. The limiting criteria for the maneuverability is the roll and pitch angles due to the limited hydrostatic restoring available on small observation class ROVs. The hydrostatic restoring in roll and pitch for the BlueROV2 can be estimated by calculating the distance between COG and COB and is found to be:

$$g_4 = 0.42 * sin(\eta_4) * cos(\eta_5) \quad (6)$$

$$g_5 = 0.42 * sin(\eta_5) \quad (7)$$

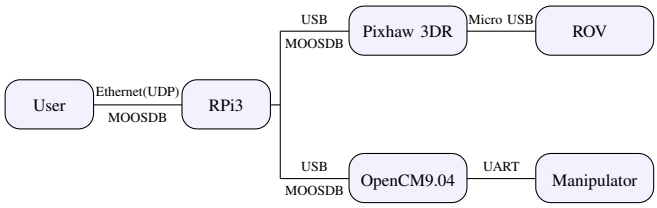

Fig. 9. Communication between user and manipulator.

where η is the position and orientation vector of the ROV.

Two basic scenarios are tested, one scenario is when the manipulator is fixed vertically and the other is when the manipulator is fixed horizontally (see Eq. (4) and (5)). Based on these two scenarios a total of four tests are performed:

- Pitch response when performing forward (surge) maneuver with the manipulator fixed vertically.
- Roll response when performing sideways (sway) maneuver with the manipulator fixed vertically.
- Pitch response when performing forward (surge) maneuver with the manipulator fixed horizontally.
- Roll response when performing sideways (sway) maneuver with the manipulator fixed horizontally.

To measure the accelerations the on board Inertial Measurement Unit (IMU) is used. Based on the accelerations the corresponding velocities are calculated using time integration. The combined vertical length of the ROV and manipulator is approximately 1 meter (with the manipulator fixed vertically) submerged operations are therefore difficult to perform without running the risk of damaging the manipulator (manipulator is mounted below the ROV). The tests performed are therefore done with the ROV located at or close to the surface. Wave generation will therefore give increased resistance of the ROV and will therefore affect the roll and pitch response as well as surge and sway.

IV. Results

This section contains the results of the experiments performed in MC-lab.

A. Surge maneuver

The surge maneuver tests were performed by applying surge thrust to the ROV and measuring the corresponding accelerations in surge and pitch. The tests were performed first by setting the manipulator in a vertical position, then with the manipulator located horizontally facing forward and lastly with the manipulator horizontally facing backwards. The results from these tests are shown in Fig. 10. Note that the surge speed is given in cm/s.

From Fig. 10 it can be seen that positioning the manipulator horizontally produces the smallest pitch response. With a vertical manipulator this oscillatory pitch motion of the ROV becomes large, while it's significantly reduced with a horizontal manipulator. Especially when the manipulator is facing backwards. The benefit of facing the manipulator backwards comes due to the fact that in this configuration

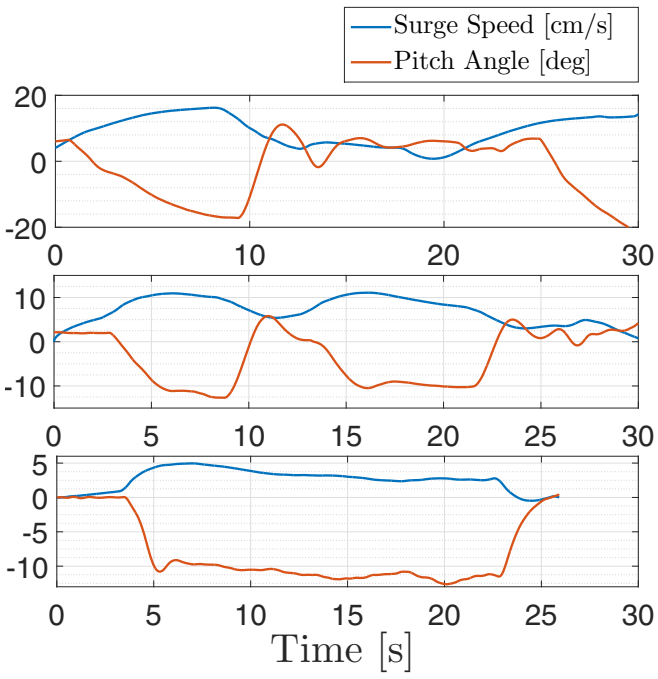

Fig. 10. ROV response with fixed manipulator during surge maneuvers. Top: manipulator fixed vertically. Mid: manipulator fixed horizontally facing forwards. Bottom: Manipulator fixed horizontally facing backwards.

a stabilizing torque is produced by the hydrodynamic forcs when ROV pitches downwards and translates in surge. In the backwards position the manipulator will hence produce a hydrodynamic restoring moment counteracting some of the hydrodynamic moment in pitch. The ROV has a larger speed during the forward configuration than during the backward configuration, but this is the result of the manual control of the ROV. It can also be seen that the surge speed drifts during the first 5 seconds of the measurements (mid and bottom). This is a result of poor IMU-performance. The IMU is of quite low quality hence time integrating the acceleration vector produces a velocity drift. The bias in the acceleration measurements is not constant hence obtaining a time series of the velocity without drift is difficult.

B. Sway maneuver

The sway tests were performed the same way as the surge tests. The results from these tests are shown in Fig. 11. It is seen from Fig. 11 that the maximum roll angle is less than 20 degrees. Although 20 degrees is a quite large angle the ROV still retains acceptable maneuverability. It can also be seen that the ROV is able to achieve a higher speed when the manipulator is oriented horizontally. It is also observed that the difference between the three scenarios (vertical, forwards and backwards facing) is much smaller than for the surge tests. This is intuitive as the manipulator is oriented perpendicular to the direction of motion for all scenarios. The largest effect on the response during the sway tests can therefore be found in the yaw rotation. The yaw rotation for the three different sway tests can be seen in Fig.

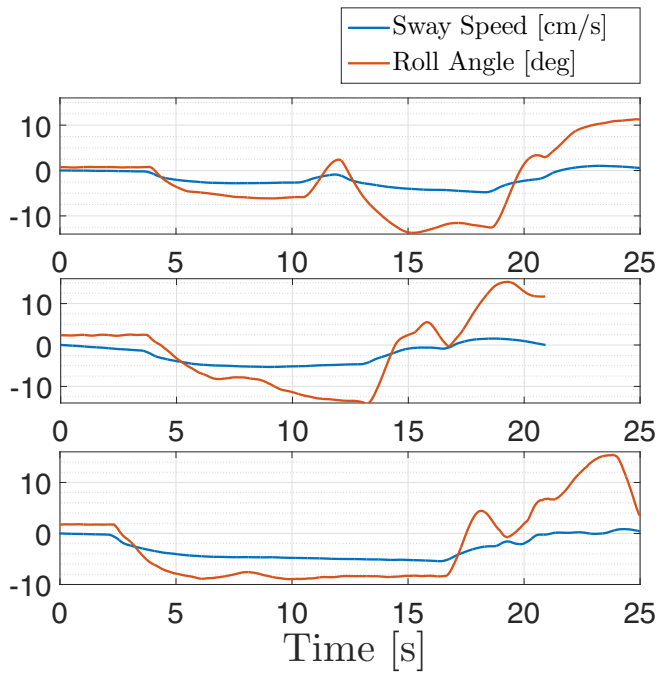

Fig. 11. ROV response with fixed manipulator during sway maneuvers. Top: manipulator fixed vertically. Mid: manipulator fixed horizontally facing forwards. Bottom: Manipulator fixed horizontally facing backwards.

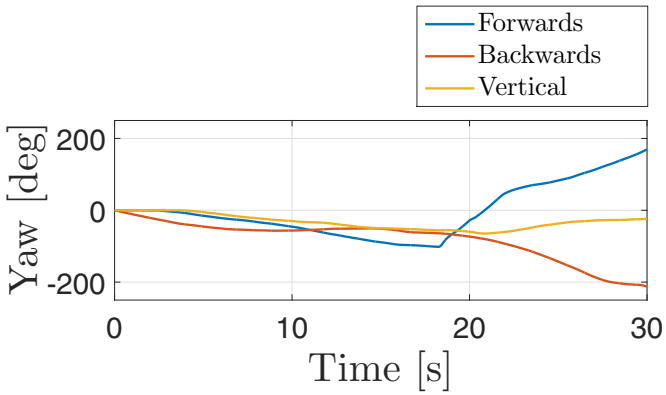

Fig. 12. ROV yaw response during sway maneuvers.

12. The manipulator produces a significant yaw rotation for the horizontal cases, but close to zero rotation for the vertical case, as expected.

V. Discussion & Conclusions

A multi degree of freedom ROV manipulator design has been presented. The manipulator is unique as it solves the complex problem of creating a manipulator that can be mounted on the smallest types of observation class ROVs. The limited amount of manipulators commercially available for small observation class ROVs today are limited to 1 or 0 (gripper) degrees of freedom and relies on accurate control of the ROV to be operated. The proposed manipulator can due to its multi degrees of freedom design perform advanced manipulation tasks using small ROVs. The manipulator is also able to counteract the response of the ROV and is therefore not dependent on extremely precise ROV control as would be the case with single or no degrees of freedom manipulators. The manipulator is also fully electric which enables a neutrally buoyant design that can be attached directly to the ROV's internal power source. Most subsea manipulators today are hydraulic which tend to create a heavy arm with relative large negative buoyancy. Hydraulic manipulators offers more torque and power, but for small scale ROVs this extra power is in many cases not needed. The manipulator presented has a stall torque of more than 8 Nm operating at 12 V. Subjecting a small observation class ROV to more than 8 Nm torque would most likely produce an undesired response in roll/pitch. The ROV itself will therefore become the limiting factor rather than the manipulator. The modular build makes the manipulator extremely versatile as it can be adjusted to fit a number of different applications. The degrees of freedom and length of the different joints can be reduced or extended easily.

From the experimental tests it is shown that the BlueROV2 is fully capable of maneuvering with the manipulator installed. When performing surge maneuvers it was shown that aligning the manipulator parallel to the direction of motion could reduce the pitch response. In sway maneuvers it was more difficult to observe what effect correctly positioning the the manipulator had on the roll response. This was most likely due to the limited sway velocity applied during the experiments. For the sway maneuvers it was however observed a large yaw rotation due to the perpendicular alignment of the manipulator relative to the direction of motion. As the maneuvers were performed manually using a joystick the different tests can not be compared directly to each other, but they prove that the ROV has no problem functioning with the manipulator installed even if the manipulator is positioned in the least desirable configuration (vertically).

VI. Further Work

Extensive testing on the ROV-manipulator system will be performed following this work. The system offers a new platform for testing and designing control systems as well as a functional platform that can be utilized in commercial and industrial use. Installation of actuation in roll and pitch can be an interesting topic to investigate. By accurately controlling the roll and pitch response the ROV-manipulator system can perform faster maneuvers and the ROV can perform more challenging tasks such as lifting heavy objects.

Perhaps the most interesting topic is to investigate the simultaneous control of the ROV and manipulator. By controlling both components the performance of the system can be drastically improved.

ACKNOWLEDGMENT

This work has been carried out at the Centre for Autonomous Marine Operations and Systems (AMOS). The Norwegian Research Council is acknowledged as the main sponsor of NTNU AMOS through the Centres of Excellence funding scheme, Project number 223254.

REFERENCES

[1] R. Christ and R. Wernli Sr., A User Guide for Remotely Operated Vehicles, Butterworth-Heinemann, 2014, 2nd Edition.

[2] Blue Robotics, BlueROV2 datasheet, Blue Robotics 2017, available at: https://bluerobotics.com/downloads/bluerov2.pdf, Accesed October 25. 2017.

[3] J. Yuh, Design and Control of Autonomous Underwater Robots: A Survey, Autonomous Robots., vol. 8(1), pp. 7-24, 2000.

[4] C. J.J Paredis, H.B. Brown and P.K. Khosla, A Rapidly Deployable Manipulator System , Proceedings of 1996 International Conference on Robotics and Automation, vol. 2, pp. 1434-1439, 1996.

[5] T. Matsumaru, Design and Control of the Modular Robot System: TOMMS., Proceedings of 1995 IEEE International Conference on Robotics and Automation, Vol. 2, pp. 2125-2131, 1995.

[6] B.U. Rehman, M. Focchi, M. Frigerio, J. Goldsmith, D. Caldwell and C. Semini , Design of a Hydraulically Actuated Arm for a Quadruped Robot, P Proceedings of the 18th International Conference on CLAWAR, pp. 283-290, 2016.

[7] F. Boyer, M. Porez and W. Khalil, Macro-Continuous Computed Torque Algorithm for a Three-Dimensional Eel-Like Robot, vol. 22(4), pp. 763-775, 2006.

[8] E. Kelasidi, K.Y. Pettersen, A.M. Kohl, J.T. Gravdahl, An Experimental Investigation of Path Following for an Underwater Snake Robot with a Caudal Fin, IFAC-PapersOnLine, 2017.

[9] M. Porez, F. Boyer and A. Ijspeert, Improved Lighthill fish swimming model for bio-inspired robots - Modelling, computational aspects and experimental comparisons, International Journal of Robotics Research, SAGE Publications, vol.33(10),pp. 1322-1341,2014

[10] P. Liljebäck, Ø. Stavdahl, K. Pettersen and J. Gravdahl, Mamba - a waterproof snake robot with tactile sensing,Procedings of the International Conference on Intelligent Robots and Systems (IROS), pp. 294-301, 2014.

[11] Robotis Inc., Robotis e-Manual v1.31.02., Robotis Inc. 2017, available at: http://support.robotis.com/en/ product/controller/opencm9.04.htm, Accesed October 25. 2017.

[12] J. Denavit and R.S. Hartenberg, A kinematic notation for lower-pair mechanisms based on matrices, Trans. of the ASME. Journal of Applied Mechanics, vol. 22, pp. 215-221, 1955.

[13] M. Benjamin, H. Schmidt and P. Newman, MOOS homepage 2017, available at: https://http://oceanai.mit.edu/ivpman/pmwiki/pmwiki.php, Accesed September 9. 2017.